Demonstration of a Switched Wideband GaN High-Power Amplifier for Future Space Missions

Rainee N. Simons, Joseph A. Downey, Bryan L. Schoenholz,
Marie T. Piasecki, and Nang T. Pham
NASA Glenn Research Center, MS 54-1
Cleveland, OH 44135, USA
Rainee.N.Simons@nasa.gov

Mansoor K. Siddiqui and Ralph G. Bonnin
Northrop Grumman Aerospace Systems
Redondo Beach, CA 90278, USA
Mansoor.Siddiqui@ngc.com

***Abstract*—In this paper, we present the architecture of a Ka-band switched, wideband, high efficiency gallium nitride based high-power amplifier. The architecture is validated by characterizing the driver and power amplifier chain. The measured results include P_{out}, Gain, PAE, RMS EVM for QPSK, Offset-QPSK, 8PSK, 16APSK, and 16QAM constellations, 3rd order IMD products, noise figure, and added phase noise. The wide bandwidth and high output power of the amplifier will enable future user terminals to interoperate between multiple service provider's space networks.**

Keywords—high power amplifier, gallium nitride, SATCOM, Ka-band, MMICs, interoperability, wideband, multi-missions

I. Introduction

NASA plans to transition in a phased manner in the next decade the NASA owned and operated near-Earth space communications capabilities to commercial SATCOM networks [1]. Hence, there is a need to evaluate commercial SATCOM capabilities that can provide high capacity, reliable, and secure near-Earth space communications services for future space missions. This requires developing terminals for user spacecraft that are capable of roaming and having performance flexibility to interoperate between multiple U.S. commercial service provider networks and space networks owned by U.S. government agencies [2]. However, these legacy systems operate over different frequency bands within the Ka-band spectrum. Therefore, there is a need to develop wideband RF/microwave components and subsystems for seamless interoperability of user terminals between space networks of multiple service providers. Additionally, NASA Artemis missions, that includes Commercial Lunar Payload Services and Lunar Gateway, in collaboration with international partners involve human/robotic exploration and long-term presence on the Moon [3]. These missions have similar interoperability requirements and would benefit from the above innovations.

In this paper, we demonstrate a Ka-band switched, wideband, high efficiency gallium nitride (GaN) monolithic microwave integrated circuit (MMIC) based high-power amplifier (HPA) for the above applications. These MMICs utilize GaN high electron mobility transistor (HEMT) technology that imparts several significant advantages over prior gallium arsenide (GaAs), Silicon Germanium (SiGe) and Silicon (Si) technologies. These include higher operating voltage, higher output power density, higher channel operating temperatures, and radiation hardness [4], [5]. GaN being a wide bandgap semiconductor, the HPA can serve as a precursor for NASA's deep space planetary missions that require communication systems to operate in the extreme hot environment of Mercury and Venus and extreme cold and high radiation environment of Jupiter's icy moons.

II. Ka-Band High Power Amplifier Architecture and Brief Set of Requirements

A brief set of requirements are as follows:

- Saturated output power (Psat) (Balanced): 17–20 watts (CW)
- Operating frequency range: 25–31 GHz
- Power added efficiency (PAE): 23–25%
- Small signal Gain (driver & power amplifier): >30 dB
- Input/output return loss: < –10.0 dB

The architecture of the Ka-band GaN HPA is illustrated in Fig. 1. In this design, the HPA's operating frequency band is split into two sub-bands, namely, 25–28 GHz and 28–31 GHz. Band splitting is necessary since a single high power MMIC chip that can operated across the entire 25–31 GHz band is not available. Each sub-band comprises of an amplifier chain that includes a pre-amplifier, driver amplifier, and a balanced power amplifier. At the HPA input, a SPDT switch routes the incoming signal, depending on the frequency, to the appropriate amplifier chain. At the HPA output, the amplified signal is routed to antennas for transmission.

III. Ka-Band High Power Amplifier Architecture Performance Validation

A. 25–28 GHz Sub-band

To demonstrate the HPA performance, a MMIC driver amplifier chip and a power amplifier chip are assembled into two modules. The modules are interconnected, and performance characterized using the Rohde & Schwarz SMW200A Vector Signal Generator, FSW Signal and Spectrum Analyzer, and Micronetics Noise Source. The measured output power (P_{out}), Gain, and PAE at the sub-band center frequency (f_0) of 26.5 GHz are presented in Fig. 2(a) and (b), respectively. The Psat is 37.7 dBm, small signal Gain is 29.6 dB, and the PAE is 18.9%. Next, to demonstrate high data rate and bandwidth efficiency, the error vector magnitude (EVM) is measured at a fixed rate of 180 Msymbols per second for the QPSK, Offset-QPSK, 8PSK, 16APSK, and 16QAM constellations that are typically used in the transmission of data in satellite communications. The results achieved are presented in Fig. 3. At the 1-dB compression point, all but the 16QAM constellation can achieve EVM of <5%. In Fig. 4, the measured 3rd order intermodulation distortion (IMD)

This manuscript is a joint work of employees of the National Aeronautics and Space Administration and employees of Northrop Grumman Systems under Order No. 80NSSC21P2024 with the National Aeronautics and Space Administration.

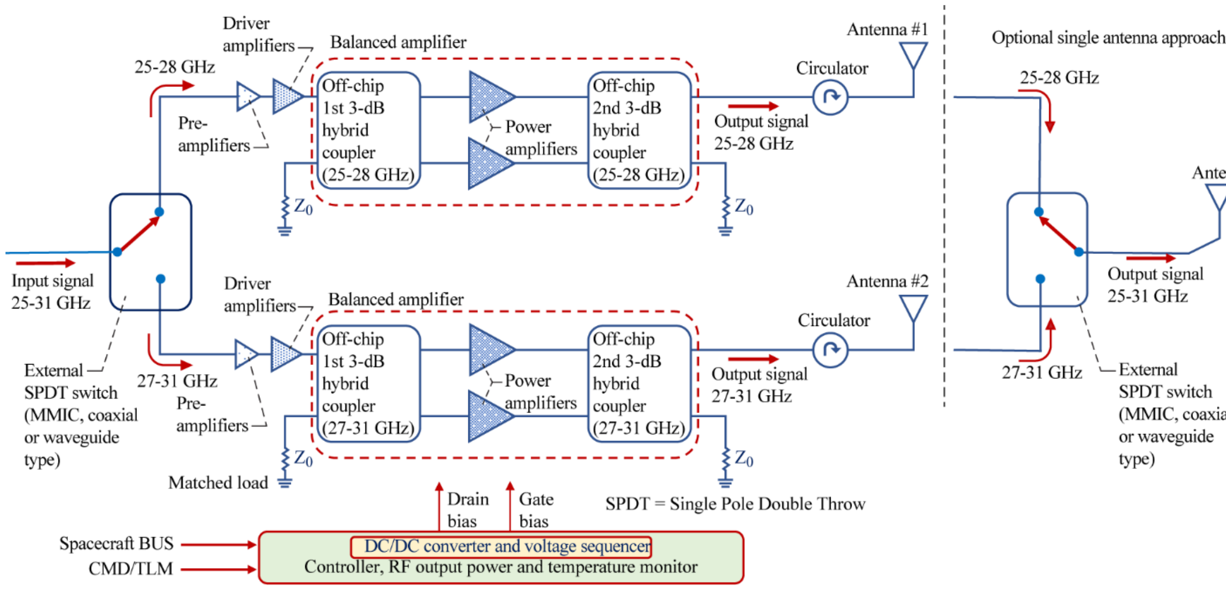

Fig. 1 GaN MMIC based Ka-band high-power amplifier (HPA) overall architecture.

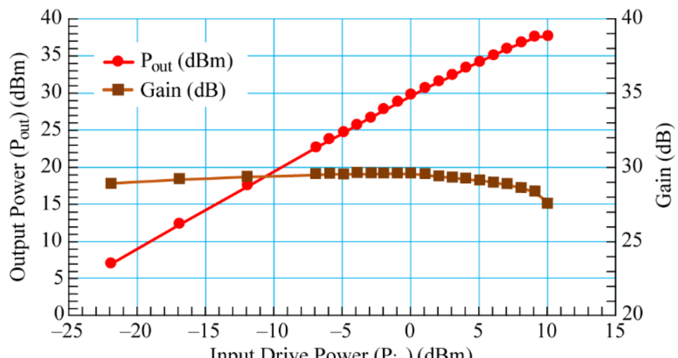

(a)

Fig. 2(a) Measured P_{out} and Gain vs. P_{in} of the interconnected driver (APN244) and power amplifiers (APN243) at sub-band f_0 of 26.5 GHz. Driver amplifier: V_d = 23.1 V and V_g = –3.9 V. Power amplifier: V_d = 23 V and V_g = –4.5 V. T = 25 °C.

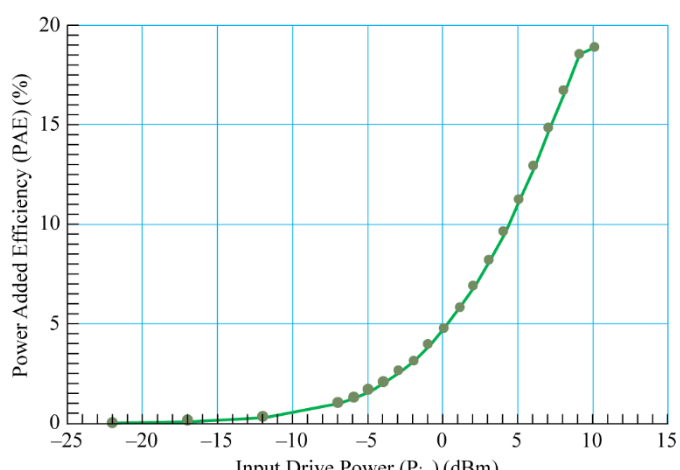

(b)

Fig. 2(b) Corresponding Measured PAE vs. P_{in}.

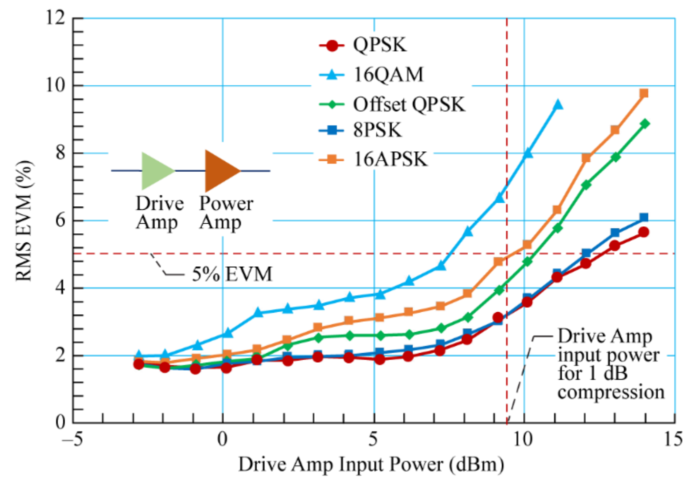

Fig. 3 Measured RMS EVM vs. P_{in} at sub-band f_0 of 26.5 GHz. The symbol rate is 180 Msymbols per second and the square root raised cosine (SRRC) filter is set to 0.35.

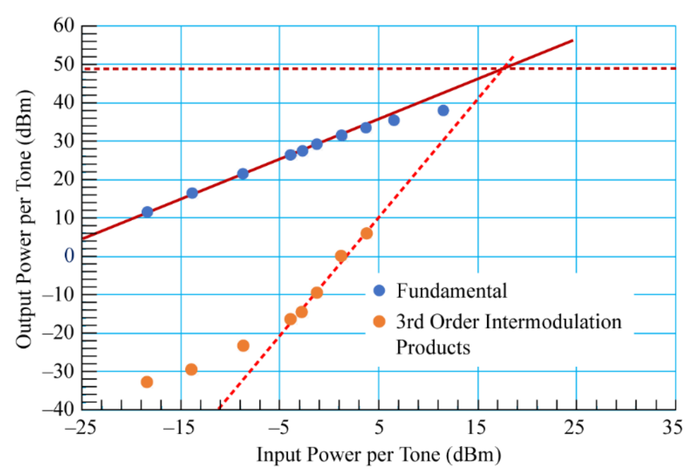

Fig. 4 Measured 3rd order intermodulation distortion (IMD) vs. input power per tone at sub-band f_0 = 26.5 GHz. Tone spacing is 5 MHz.

products are presented to demonstrate good linearity. The data indicates that the output 3rd order intercept point (OIP3) is 48 dBm. The measured noise figure (NF) is presented in Fig. 5. The NF is less than 9 dB across the 25–28 GHz sub-band. The NF is slightly higher than expected because of a series resistor in the gate circuit for stabilization.

B. 28–31 GHz Sub-band

The measured P_{out}, Gain, and PAE are presented in Fig. 6(a) and (b), respectively. The Psat is 38.4 dBm, small signal Gain is 31.4 dB, and the PAE is 23.3%. The measured EVM at a fixed rate of 180 Msymbols per second for the QPSK, Offset-QPSK, 8PSK, 16APSK, and 16QAM constellations are presented in Fig. 7. At the 1-dB compression point, the EVM for QPSK and 8PSK constellations is less than 5%. As an example, the measured spectrum of the 16APSK waveform is presented in Fig. 8. For this measurement, the drive amp input power is backed-off slightly from the 1-dB compression point so that the EVM is less than 5%. The out-of-band spectral regrowth is less than 30 dB and compliant with the NTIA emission mask. The 3rd order IMD products are measured and the results are presented in Fig. 9. The OIP3 is 53 dBm. The measured NF is presented in Fig. 10. The NF is less than 7 dB across the 27–31 GHz sub-band. The above set of MMIC amplifiers operate down to 27 GHz. The 1 GHz overlap while providing redundancy and back-up enhances reliability for the 25–28 GHz sub-band extensively used for NASA's communications. The measured single sideband (SSB) added phase noise at the 1-dB compression point and at the two sub-band center frequencies are presented in Fig. 11(a) and (b), respectively. The SSB phase noise power spectral density is in complaint with the envelope defined in the MIL-STD-188-164C.

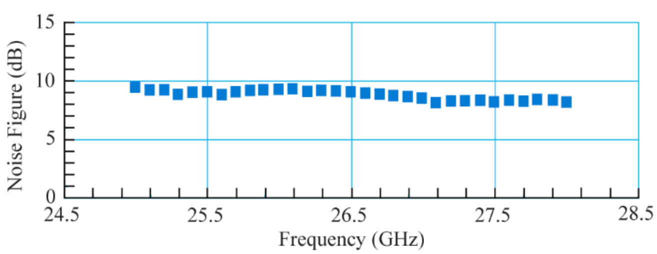

Fig. 5 Measured noise figure vs. frequency.

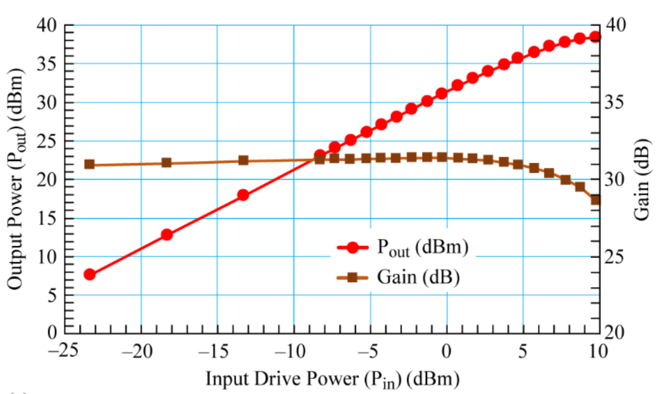

(a)

Fig. 6(a) Measured P_{out} and Gain vs. P_{in} of the interconnected driver (APN229) and power amplifiers (APN228) at sub-band f_0 of 29.5 GHz. Driver amplifier: V_d = 21 V and V_g = –4.5 V. Power amplifier: V_d = 21 V and V_g = –4.65 V. T = 25 °C.

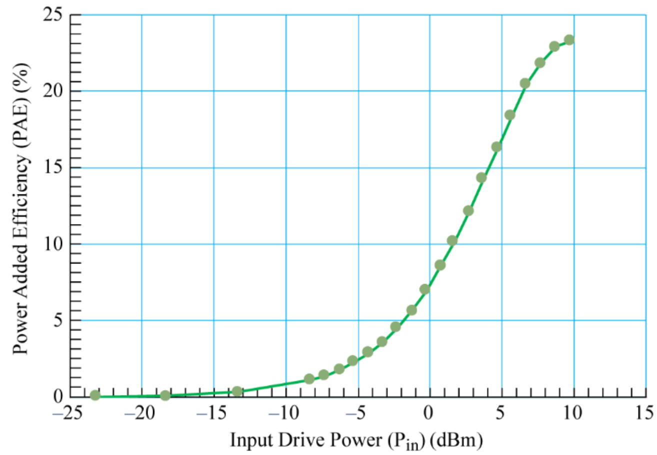

(b)

Fig. 6(b) Corresponding Measured PAE vs. P_{in}.

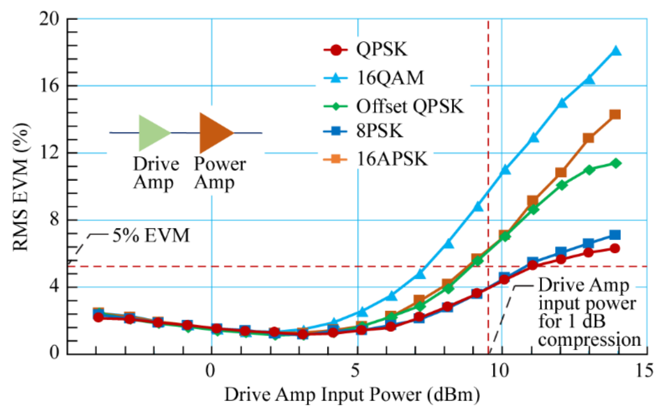

Fig. 7 Measured RMS EVM vs. P_{in} at sub-band f_0 of 29.5 GHz. The symbol rate is 180 Msymbols per second and the SRRC filter is set to 0.35.

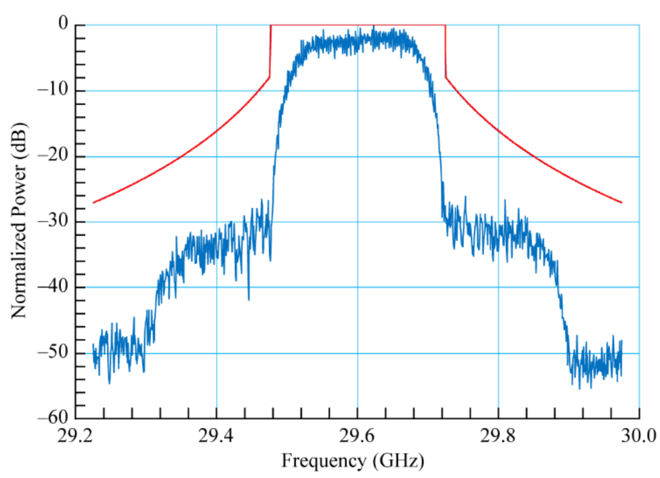

Fig. 8 Measured spectrum of the 16APSK waveform. Carrier frequency is 29.6 GHz, symbol rate is 180 Msymbols per second, SRRC filter is set to 0.35. The red solid line is the NTIA emission mask. Bandwidth is 250 MHz.

CONCLUSIONS AND DISCUSSIONS

The advantages of GaN for NASA's space applications is highlighted. The architecture and design of a Ka-band GaN HEMT based MMIC HPA is discussed. The architecture is validated by characterizing interconnected driver and power amplifier modules. The measured P_{out}, Gain, PAE, RMS EVM

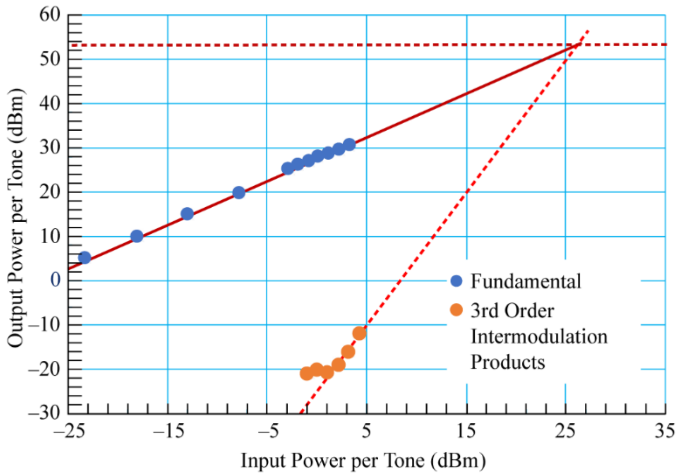

Fig. 9 Measured 3rd order intermodulation distortion (IMD) vs. input power per tone at sub-band f_0 = 29.5 GHz. Tone spacing is 5 MHz.

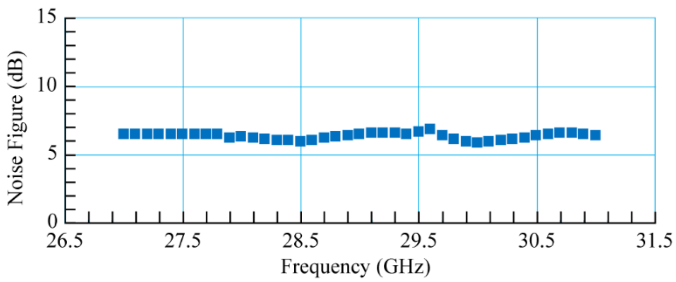

Fig. 10 Measured noise figure vs. frequency.

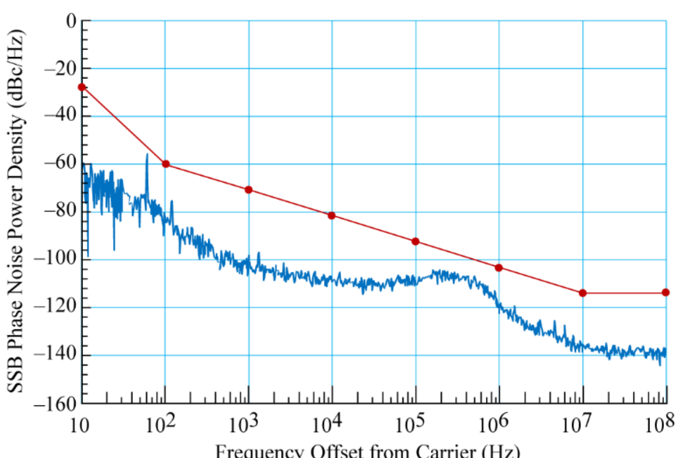

(a)

Fig. 11(a) Measured SSB added phase noise at sub-band f_0 of 26.5 GHz. The red solid line is the MIL-STD-188-164C mask.

for QPSK, Offset-QPSK, 8PSK, 16APSK, and 16QAM constellations, 3rd order IMD products, noise figure, and added phase noise are presented and summarized in Table I. GaN HEMTS enable higher power density, higher PAE resulting in lighter, smaller, and more efficient RF/microwave systems in contrast with Si, SiGe, and GaAs based systems.

Acknowledgment

The authors would like to thank the Space Communications and Navigation (SCaN) Program for the support.

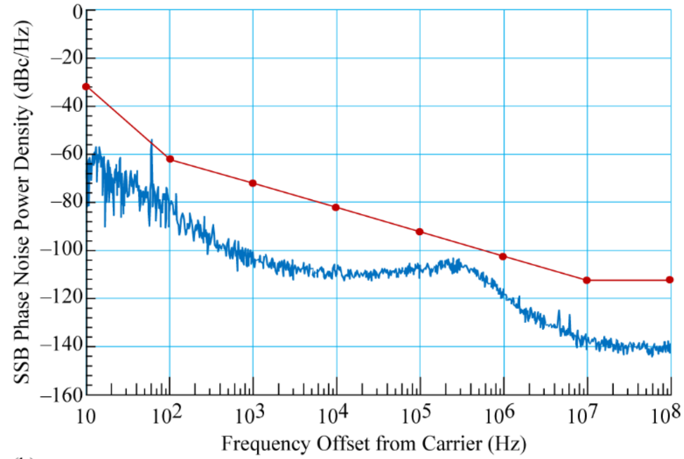

(b)

Fig. 11(b) Measured SSB added phase noise at sub-band f_0 of 29.5 GHz. The red solid line is the MIL-STD-188-164C mask.

TABLE I. Test Results Summary

Parameter	Measured Value (25–28 GHz Driver & Power Amp)	Measured Value (28–31 GHz Driver & Power Amp)
Output Power (dBm) (Sat)	37.7	38.4
Small Signal Gain (dB)	29.6	31.4
PAE (%)	18.9	23.3
Return Loss (dB)	< –10.0	< –10.0
EVM (%) (drive at 1-dB compression point) (QPSK, Offset-QPSK, 8PSK, 16APSK, & 16QAM)	5 (All but 16QAM) 7 (16QAM)	5 (QPSK & 8PSK) 6 (Offset-QPSK & 16APSK) 10 (16QAM)
Out-of-Band Spectral Regrowth (dB)	< 30	< 30
OIP3 (dBm)	48	53
Noise Figure (dB)	9 (Higher NF due to stabilizing gate resistor)	7
SSB Phase Noise Power Density (dBc/Hz) (drive at 1-dB compression point)	Compliant with MIL-STD Mask Added Phase Noise is insignificant	Compliant with MIL-STD Mask Added Phase Noise is insignificant

References

[1] SCaN the future: a virtual event—proceedings, Oct 29, 2020, https://www.nasa.gov/directorates/heo/scan/services/scan_the_future_proceedings.

[2] M. Piasecki, J. Downey, N. Pham, J. Nessel, A. Gannon, D. Zeleznikar, and M. Koch, "Development and demonstration of a wideband rf user terminal for roaming between ka-band relay satellite networks," *38th Inter Communications Satellite Systems Conf (ICSSC 2021)*, Arlington, VA, Sept 27–30, 2021, doi: 10.1049/icp.2022.0579.

[3] Artemis Program, https://www.nasa.gov/artemisprogram.

[4] S. Din, M. Wojtowicz and M. Siddiqui, "High power and high efficiency ka band power amplifier," *IEEE MTT-S Inter. Micro Symp Dig*, Phoenix, AZ, May 17–22, 2015.

[5] S. Din, A.M. Morishita, N. Yamamoto, C. Brown, M. Wojtowicz, and M. Siddiqui, "High-power k-band GaN pa mmics and module for npr and pae," *IEEE MTT-S Inter. Micro Symp Dig*, Honolulu, HI, June 4–9, 2017.